

The top induced backgrounds to Higgs production in the $WW^{(*)} \rightarrow ll\nu\nu$ decay channel at NLO in QCD

R. Frederix

PH Department, TH Unit, CERN, CH-1211 Geneva 23, Switzerland

We present the complete NLO contributions to the $pp \rightarrow e^+\nu_e\mu^-\bar{\nu}_m b\bar{b} + X$ process in the four flavour scheme, i.e. with massive b quarks, and its contribution to the $H \rightarrow WW^{(*)} \rightarrow ll\nu\nu$ measurement in the 1-jet bin at the LHC. This background process includes top pair, single top and non-top quark-resonant contributions. The uncertainty at NLO from renormalisation and factorisation scale dependence is about $+30\% -20\%$. We show that the NLO corrections are relatively small, and that separating this background in top pair, Wt and b -quark associated $ll\nu\nu$ is a fair approximation.

For the recent discovery of the Higgs boson the most important channels are the $H \rightarrow \gamma\gamma$, $H \rightarrow ZZ^{(*)} \rightarrow 4l$ and $H \rightarrow WW^{(*)} \rightarrow ll\nu\nu$ decay modes [1, 2]. Even though the latter has the largest branching ratio, it has the smallest contribution to the Higgs signal significance. This comes as no surprise: due to the presence of two neutrinos in the final state, the reconstruction of the Higgs signal in the form of a narrow resonance peak over a flat background is not possible for this decay mode. This makes the separation of the Higgs signal from (non) reducible backgrounds much more complicated and precise predictions for the backgrounds are needed to determine the excess of events that can be attributed to the Higgs signal.

To increase the significance in the extraction of the Higgs contribution for the $H \rightarrow WW^{(*)} \rightarrow ll\nu\nu$ channel, the data is separated in jet bins by the CMS and ATLAS experiments [3, 4]. In the 0-jet bin, the dominant background is the non-reducible $pp \rightarrow WW$ production. In the 1-jet bin, where each event is required to have exactly 1 jet in association with the two charged leptons and the missing E_T , also the backgrounds from top quarks are large; mostly top pair and Wt production. For a reliable simulation of these backgrounds, including next-to-leading order (NLO) QCD corrections in the calculation is essential. In this letter, we present the top induced background to Higgs production in the 1-jet bin, without separating top pair and Wt production and thus keeping all their interference effects. This requires the calculation of the NLO corrections to the $pp \rightarrow e^+\nu_e\mu^-\bar{\nu}_m b\bar{b} + X$ process in the four-flavour (4F) scheme, keeping the b quark mass finite, which we present here for the first time.

The NLO corrections to the $pp \rightarrow e^+\nu_e\mu^-\bar{\nu}_m b\bar{b} + X$ process in the *five-flavour (5F) scheme* are known [5–7]. In the 5F scheme the mass of the b quark is neglected, which means that the above process is not finite in fixed-order perturbation theory without requiring phase-space cuts on the final state b jets. Therefore, such a calculation is not a complete description of the Wt and top pair production processes and, moreover, it cannot be used to estimate the top background in the 1-jet bin in the $H \rightarrow WW^{(*)} \rightarrow ll\nu\nu$ measurement, where a veto on a second jet is needed.

The calculation of the $pp \rightarrow e^+\nu_e\mu^-\bar{\nu}_m b\bar{b} + X$ process in the 4F scheme includes double top-quark resonant production (“top pair production”), single top-quark resonant contributions (“ W boson associated single top production”) as well as non top-quark resonant contributions (“ b -quark associated $ll\nu\nu$ production”). In Fig. 1 three representative LO Feynman diagrams are shown for this process. The calculation includes all the interference effects between the various contributions, as well as all off-shell effects. In the 4F scheme the b quarks are treated as massive particles, the running of the strong coupling is performed with four flavours and a 4F PDF set should be used. Keeping the b quark massive in the calculation implies that even in the absence of any phase-space cuts, the perturbative expansion yields finite results. For the NLO computation presented here, the complete $\mathcal{O}(\alpha_s)$ corrections have been included without resorting to any approximations.

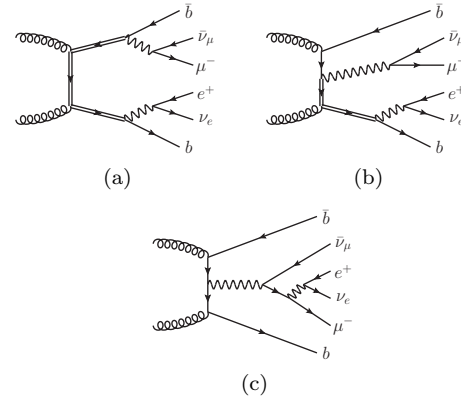


FIG. 1: Representative LO diagrams for top pair (a), Wt (b) and b -quark associated $ll\nu\nu$ (c) contributions to $pp \rightarrow e^+\nu_e\mu^-\bar{\nu}_m b\bar{b} + X$ production. Top quarks are denoted by double fermion lines.

The calculation has been performed within the MADGRAPH5_AMC@NLO framework [8]: the diagram generation is done by MADGRAPH [9], the one-loop corrections are obtained with MADLOOP [10], which is based on the OPP reduction method [11] and its implementation in CUTTOOLS [12]. The phase-space integration

and the cancellation of IR divergences in intermediate steps of the calculation are dealt with by MADFKS [13], which is based on the FKS subtraction method [14]. Furthermore, we use the complex mass scheme [15, 16], as implemented in MADGRAPH5_AMC@NLO [17], for the treatment of the widths of heavy resonances. The implementation of the various contributions in the MADGRAPH5_AMC@NLO program is done in a completely process-independent way and allows for complete automation of the calculation with extensively tested algorithms, which minimises the possibility of computational errors.

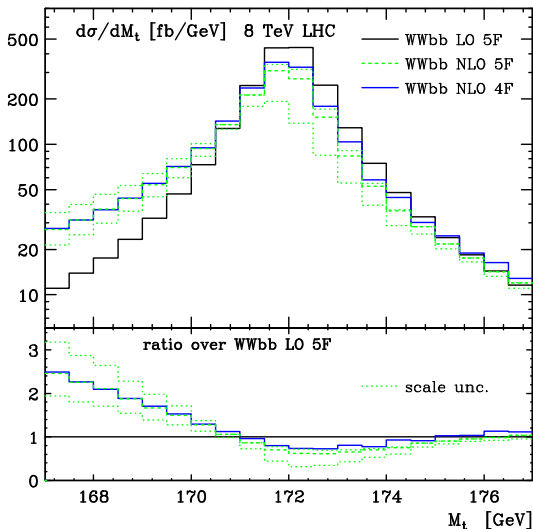


FIG. 2: Top quark invariant mass computed by taking the invariant mass of the positron, electron-neutrino and the jet containing the b quark, using the same parameters and cuts as in Ref. [7] for the $pp \rightarrow e^+ \nu_e \mu^- \bar{\nu}_\mu b\bar{b} + X$ process. The LO (black solid) and NLO (green dashed) predictions in the 5F scheme and NLO in the 4F scheme (blue solid) are plotted. The green dotted lines show the scale uncertainty on the NLO 5F result.

As a further check on the implementation of the various algorithms in the MADGRAPH5_AMC@NLO program, we have compared the results obtained in the 5F scheme by Denner *et al.* in Ref. [7] by a 5F scheme calculation obtained within our framework and found excellent agreement. As an example, in Fig. 2 we show the positron-electron-neutrino- b -jet invariant mass, using exactly the same cuts and parameters as used in Ref. [7]; thus this plot can be directly compared to Fig. 16 of that reference. In the plot, we also present the same observable simulated in the 4F scheme, i.e. the calculation presented for the first time in this letter. The 4F and 5F scheme results lie (almost) exactly on top of each other for $M_t < 172$ GeV, where the shape is dominated by resonant contributions ($M_t \simeq 172$ GeV) in which some radiation from the bottom quark is not clustered in the b jet. The region $M_t > 172$ GeV is more sensitive to the exact treatment of the (non)-resonant contributions [18], but

also here the differences between 4F and 5F scheme calculation are small and their respective scale uncertainty bands overlap. (Uncertainty band for the 4F scheme calculation is not shown).

To predict the top induced backgrounds in the $H \rightarrow WW^{(*)} \rightarrow ll\nu\nu$ decay channel at the 8 TeV LHC we use the following parameters. The mass of the top quark is set to $m_t = 172$ GeV, the mass of the bottom quark is $m_b = 4.7$ GeV and the mass of the W and Z bosons are $m_W = 80.399$ GeV and $m_Z = 91.188$ GeV. The (inverse of the) weak coupling is set to $\alpha^{-1} = 132.35$. The width of the W and Z bosons are $\Gamma_W = 2.100$ GeV and $\Gamma_Z = 2.510$ GeV, respectively. At LO the top width is set to $\Gamma_t^{\text{LO}} = 1.44$ GeV and at NLO we use $\Gamma_t^{\text{NLO}} = 1.32$ GeV. For the description of the partons inside the colliding protons, the 4F MSTW2008nf4(N)LO PDF sets [19] are used for the (N)LO calculation. This also defines the numerical value and running of the strong coupling constant.

We impose the following “Higgs measurement” cuts on the final state particles, which are motivated by the cut-based analysis for the ATLAS measurement of the Higgs boson in the $WW^{(*)} \rightarrow ll\nu\nu$ decay channel [4]. We require two charged leptons in the central rapidity region, $|\eta_l| < 2.4$, of which the hardest needs to have a transverse momentum $p_T^{\text{lead}} > 25$ GeV and the other a $p_T^{\text{sublead}} > 15$ GeV. The lepton invariant mass should be larger than $m_{ll} > 10$ GeV. We require exactly one jet with $|\eta_j| < 4.7$, defined using the anti- k_T algorithm [20] with $\Delta R = 0.5$ and a minimal transverse energy of $E_T^j > 30$ GeV, where $E_T = \sqrt{m^2 + p_T^2}$. Furthermore, there should be a sizeable (relative) missing transverse energy $E_{T,\text{rel}}^{\text{miss}} > 25$ GeV, where $E_{T,\text{rel}}^{\text{miss}} = s E_T^{\text{miss}}$, with E_T^{miss} the usual missing transverse energy and $s = \sin |\Delta\phi_{\text{closest}}|$, i.e. the sinus of the azimuthal separation between the missing transverse momentum vector and the closest charged lepton or the jet if there is one in the same azimuthal hemisphere. If there is no such object, $s = 1$. The MC truth is used to define the missing transverse energy vector as the (transverse part of the) sum of the two neutrino momenta. Finally, the following $H \rightarrow WW^{(*)} \rightarrow ll\nu\nu$ topology cuts are applied: the lepton invariant mass should be smaller than $m_{ll} < 50$ GeV and their azimuthal separation smaller than $|\Delta\phi_{ll}| < 1.8$.

Due to the complexity of the process, and the rather involved set of cuts, it is not straight-forward to define a single hard scale for this process that could be used as a renormalisation and factorisation scale. We have therefore chosen a scale that is not very specific to this process, but should capture well the general hardness of the kinematics. This central scale is $\mu_R^0 = \mu_F^0 = H_T/2$, i.e. half the scalar sum of the transverse energies of all the final state particles/partons (including the two neutrinos). With this central scale, NLO corrections are relatively small for both the inclusive process as well as after applying the cuts

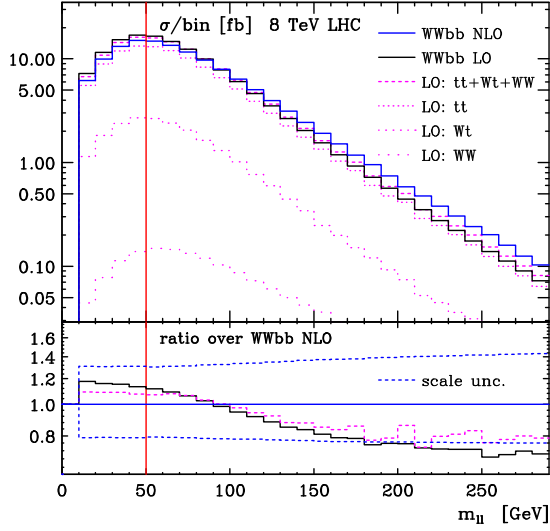


FIG. 3: Invariant mass of the charged lepton pair for the $pp \rightarrow e^+ \nu_e \mu^- \bar{\nu}_m b \bar{b} + X$ process in the 4F scheme, with the Higgs measurement cuts, apart from the cut on the charged lepton invariant mass $m_{ll} < 50$ GeV.

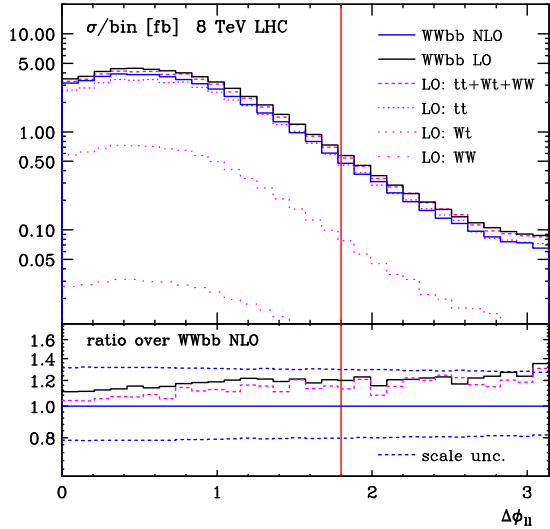


FIG. 4: Azimuthal separation of the charged leptons for the $pp \rightarrow e^+ \nu_e \mu^- \bar{\nu}_m b \bar{b} + X$ process in the 4F scheme, with the Higgs measurement cuts, apart from the cut on the charged lepton invariant mass $|\Delta\phi_{ll}| < 1.8$.

described above. To assess contributions from beyond NLO we assign an uncertainty to our predictions by computing the envelope of the results with renormalisation and factorisation scales equal to $(\mu_R, \mu_F) = \{(1, 1), (0.5, 0.5), (2, 2), (0.5, 1), (2, 1), (1, 0.5), (1, 2)\} \times (\mu_R^0, \mu_F^0)$. These 7 values are obtained at no extra CPU cost using the reweighting method described in Ref. [21].

In Figs. 3-5 we show the invariant mass of the two charged leptons (m_{ll}), the azimuthal separation of the two leptons ($\Delta\phi_{ll}$) and the transverse mass of the Higgs boson (m_T^H), respectively. The latter is defined as

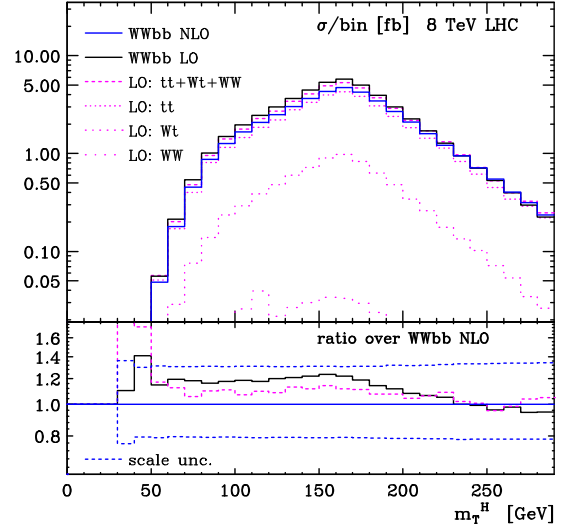


FIG. 5: Higgs transverse mass for the $pp \rightarrow e^+ \nu_e \mu^- \bar{\nu}_m b \bar{b} + X$ process in the 4F scheme, with the Higgs measurement cuts.

$m_T^H = \sqrt{(E_T^{ll} + E_T^{\text{miss}})^2 - |\mathbf{p}_T^{ll} + \mathbf{E}_T^{\text{miss}}|^2}$, where $E_T^{ll} = \sqrt{|\mathbf{p}_T^{ll}|^2 + m_{ll}^2}$. The m_{ll} and $\Delta\phi_{ll}$ variables are used to define the ‘‘Higgs topology’’ cuts, while the m_T^H distribution is used to extract the Higgs signal in the cut-based analysis by ATLAS [4]. In the plots, results for the full $pp \rightarrow e^+ \nu_e \mu^- \bar{\nu}_m b \bar{b} + X$ process at LO (labelled ‘‘WWbb LO’’) and NLO (‘‘WWbb NLO’’) are presented. Also shown are the separate LO calculations for top pair production (‘‘LO: tt’’), W -boson associated single top production (‘‘LO: Wt’’), b -quark associated $ll\nu\nu$ production (‘‘LO: WW’’) and their sum (‘‘LO: tt+Wt+WW’’). These latter processes are defined in the narrow width approximation, i.e. in the LO: tt process we take only diagrams with two s-channel top quark propagators into account (e.g. Fig. 1(a)), LO: Wt has only diagrams with one s-channel top quark propagator (e.g. Fig. 1(b)), while the LO: WW process has no s-channel top quark propagators in any of its contributing diagrams (e.g. Fig. 1(c)); all other parameters are the same as used for the WWbb LO predictions. The differences between the LO: tt+Wt+WW and WWbb LO results stem only from interference effects (among the three contributions to the LO: tt+Wt+WW prediction) which are only included in the complete WWbb simulations. For the m_{ll} and $\Delta\phi_{ll}$ plots, the Higgs topology cut on that distribution is not applied, and is denoted by the vertical line. In the lower inset of the plots, the ratio is taken w.r.t. the WWbb NLO result. Also shown here is the relative scale uncertainty on the NLO result. For the observables studied here, LO scale uncertainties are marginally larger than the NLO scale uncertainties. We refrain from showing these, because scale uncertainties at LO are not a proper estimate of missing higher order corrections, in particular when jet veto’s are applied or when studying exclusive jet bins, as is done here.

As can be seen from the plots, the NLO corrections are small and negative (about -20%) when all the cuts are applied. This is within the NLO scale uncertainty, which is about +30% -20%. It is no surprise that the scale dependence at NLO is still sizeable because the observables considered are rather exclusive; particularly due to the veto of any jets beyond the hardest. There is a visible difference in shape between the LO and NLO results, even though it stays within the NLO scale uncertainties. This difference in shape in the m_{ll} distribution is of particular importance, because the region at large invariant mass, $m_{ll} > 80$ GeV, is used as a background control sample in the ATLAS analysis.

When summing the separate LO calculations for $t\bar{t}$, Wt and b -quark included WW production, the final result is very close to the $WWbb$ LO prediction. The bulk is given by top pair production, Wt being about a factor 5 smaller and the contribution from b -quark associated WW production is approximately 2 orders of magnitude smaller than top pair production. Interesting to see is that the sum of the separate calculations lies in between the LO and NLO $WWbb$ results. This is not only the case for the 3 observables presented here, but seems to be a general feature of this process. Most likely, this is due to positive interference effects between $t\bar{t}$ and Wt production, which results in a slightly higher cross section when these effects are taken into account. On top of that, the NLO corrections bring the results down again, slightly below the LO result without interference effects.

To conclude, we have presented a calculation of the the top quark induced backgrounds to the $H \rightarrow WW^{(*)} \rightarrow ll\nu\nu$ measurement in the 1-jet bin by computing the NLO corrections to the process $pp \rightarrow e^+\nu_e\mu^-\bar{\nu}_\mu b\bar{b} + X$ in the four-flavour scheme. This process yields a consistent description of top pair production, W -boson associated single top production and b -quark associated WW production, including all interference and off-shell effects. Using $H_T/2$ as a central renormalisation and factorisation scale, the NLO corrections are small and negative in the Higgs signal region and its uncertainties from renormalisation and factorisation scale dependence are about +30% -20%. There is, however, a difference in shape between LO and NLO in the m_{ll} distribution: the negative NLO corrections at small m_{ll} (Higgs signal region) turn positive for large m_{ll} , which is the background control region. Therefore, this might have an affect on the recent Higgs boson measurements. Using separate calculations for $t\bar{t}$ and Wt (and b -quark associated WW) production based on the narrow width approximation for the top quark, yields a fair approximation of the final results, within left-over theoretical uncertainties.

For a more exclusive description of the final state, matching to the parton shower would be required. This would allow for an improved description of the jets, in particular when b -tagging would be applied, and a fair comparison to the data can be made. When matching

to the parton shower using the MC@NLO technique [22], care has to be taken to prevent double counting from the NLO corrections and parton shower (non-)emissions from the intermediate top quarks. Work in this direction has already been started.

I would like to thank V. Hirschi for writing the `virt_reweight.py` code that has been used to obtain and check some parts of the results presented here. I also thank S. Frixione, F. Maltoni, V. Hirschi, O. Mattelaer, M. Zaro and P. Torrielli for proof-reading this manuscript.

-
- [1] G. Aad et al. (ATLAS Collaboration), Phys.Lett. **B716**, 1 (2012), 1207.7214.
 - [2] S. Chatrchyan et al. (CMS Collaboration), Phys.Lett. **B716**, 30 (2012), 1207.7235.
 - [3] S. Chatrchyan et al. (CMS Collaboration), Phys.Lett. **B710**, 91 (2012), 1202.1489.
 - [4] Tech. Rep. ATLAS-CONF-2013-030, CERN, Geneva (2013).
 - [5] A. Denner, S. Dittmaier, S. Kallweit, and S. Pozzorini, Phys.Rev.Lett. **106**, 052001 (2011), 1012.3975.
 - [6] G. Bevilacqua, M. Czakon, A. van Hameren, C. G. Papadopoulos, and M. Worek, JHEP **1102**, 083 (2011), 1012.4230.
 - [7] A. Denner, S. Dittmaier, S. Kallweit, and S. Pozzorini, JHEP **1210**, 110 (2012), 1207.5018.
 - [8] R. Frederix, S. Frixione, V. Hirschi, F. Maltoni, O. Mattelaer, T. Stelzer, P. Torrielli, and M. Zaro, *in preparation*.
 - [9] J. Alwall, M. Herquet, F. Maltoni, O. Mattelaer, and T. Stelzer, JHEP **1106**, 128 (2011), 1106.0522.
 - [10] V. Hirschi, R. Frederix, S. Frixione, M. V. Garzelli, F. Maltoni, and R. Pittau, JHEP **05**, 044 (2011), 1103.0621.
 - [11] G. Ossola, C. G. Papadopoulos, and R. Pittau, Nucl. Phys. **B763**, 147 (2007), hep-ph/0609007.
 - [12] G. Ossola, C. G. Papadopoulos, and R. Pittau, JHEP **03**, 042 (2008), 0711.3596.
 - [13] R. Frederix, S. Frixione, F. Maltoni, and T. Stelzer, JHEP **10**, 003 (2009), 0908.4272.
 - [14] S. Frixione, Z. Kunszt, and A. Signer, Nucl. Phys. **B467**, 399 (1996), hep-ph/9512328.
 - [15] A. Denner, S. Dittmaier, M. Roth, and D. Wackeroth, Nucl.Phys. **B560**, 33 (1999), hep-ph/9904472.
 - [16] A. Denner, S. Dittmaier, M. Roth, and L. H. Wieders, Nucl. Phys. **B724**, 247 (2005), hep-ph/0505042.
 - [17] D. Buarque Franzosi, V. Hirschi, and O. Mattelaer, *in preparation*.
 - [18] A. Papanastasiou, R. Frederix, S. Frixione, V. Hirschi, and F. Maltoni, Phys.Lett. **B726**, 223 (2013), 1305.7088.
 - [19] A. Martin, W. Stirling, R. Thorne, and G. Watt, Eur.Phys.J. **C63**, 189 (2009), 0901.0002.
 - [20] M. Cacciari, G. P. Salam, and G. Soyez, JHEP **0804**, 063 (2008), 0802.1189.
 - [21] R. Frederix, S. Frixione, V. Hirschi, F. Maltoni, R. Pittau, and P. Torrielli, JHEP **1202**, 099 (2012), 1110.4738.
 - [22] S. Frixione and B. R. Webber, JHEP **06**, 029 (2002), hep-ph/0204244.